Title

Novel large-particle FACS purification of adult ventricular myocytes reveals accumulation of myosin and actin disproportionate to cell size and proteome in normal post-weaning development

Authors

López, Javier E
Sharma, Janhavi
Avila, Jorge
et al.

Publication Date

2017-10-01

DOI

10.1016/j.yjmcc.2017.07.012

Peer reviewed

HHS Public Access

Author manuscript

J Mol Cell Cardiol. Author manuscript; available in PMC 2018 October 01.

Published in final edited form as:

J Mol Cell Cardiol. 2017 October ; 111: 114–122. doi:10.1016/j.yjmcc.2017.07.012.

Novel Large-Particle FACS Purification of Adult Ventricular Myocytes Reveals Accumulation of Myosin and Actin Disproportionate to Cell Size and Proteome in Normal Post-weaning Development

Javier E. López, MD, MAS[a], **Janhavi Sharma, PhD**[a], **Jorge Avila, BS**[a], **Taylor S. Wood, BS**[a], **Jonathan Van Dyke, BS**[a], **Bridget Mclaughlin, MS**[a], **Craig Abbey, PhD**[b], **Andrew Wong, BS**[a], **Bat-Erdene Myagmar, MD, PhD**[c], **Philip M. Swigart, MS**[c], **Paul C. Simpson, MD**[c], and **Nipavan Chiamvimonvat, MD**[a,d]

[a]University of California, Davis

[b]University of California, Santa Barbara

[c]VA Medical Center, and University of California, San Francisco, CA

[d]VA Medical Center, Mather, CA

Abstract

Rationale—Quantifying cellular proteins in ventricular myocytes (MCs) is challenging due to tissue heterogeneity and the variety of cell sizes in the heart. In post-weaning cardiac ontogeny, rod-shaped MCs make up the majority of the cardiac mass while remaining a minority of cardiac cells in number. Current biochemical analyses of cardiac proteins do not correlate well the content of MC-specific proteins to cell type or size in normally developing tissue.

Objective—To develop a new MC-specific large-particle fluorescent-activated cell sorting (LP-FACS) strategy for the purification of adult rod-shaped MCs. This approach is developed to enable growth-scaled measurements per-cell of the MC proteome and sarcomeric protein (i.e. myosin heavy chain (MyHC) and alpha-actin (α-actin)) content.

Methods and Results—Individual cardiac cells were isolated from 21-94 days old mice. An LP-FACS jet-in-air system with a 200-μm nozzle was defined by the first time to purify adult MCs. Cell-type specific immunophenotyping and sorting yielded ≥95% purity of adult MCs independently of cell morphology and size. This approach excluded other cell types and tissue contaminants from further analysis. MC proteome, MyHC and α-actin proteins were measured in linear biochemical assays normalized to cell numbers. Using the allometric coefficient α, we

Address correspondence to: Javier E. López, MD, MAS, Cellular and Molecular Cardiology, 451 E. Health Science Dr., GBSF Suite #6303, Davis CA 95616, drilopez@ucdavis.edu.

DISCLOSURES

None

scaled the MC-specific rate of protein accumulation to growth post-weaning. MC-specific volumes (α=1.02) and global protein accumulation (α=0.94) were proportional (i.e. isometric) to body mass. In contrast, MyHC and α-actin accumulated at a much greater rate (i.e. hyperallometric) than body mass (α= 1.79 and 2.19 respectively) and MC volumes (α= 1.76 and 1.45 respectively).

Conclusion—Changes in MC proteome and cell volumes measured in LP-FACS purified MCs are proportional to body mass post-weaning. Oppositely, MyHC and α-actin are concentrated more rapidly than what would be expected from MC proteome accumulation, cell enlargement, or animal growth alone. LP-FACS provides a new standard for adult MC purification and an approach to scale the biochemical content of specific proteins or group of proteins per cell in enlarging MCs.

Keywords

single-cell analysis; myosin heavy chain; α-actin; cell size; proteostasis; FACS

INTRODUCTION

Cardiac tissue heterogeneity and extracellular matrix (ECM) composition complicate linking protein changes during normal myocyte (MC) growth (i.e. ontogeny) or hypertrophy to specific cell types. Adult ventricular tissues are normally composed of non-muscle cells (NMCs) and MCs in a 2:1 ratio[1]. Hence, accounting for specific changes in cellular proteins during cardiac ontogeny or disease is challenging if tissue sampling does not reflect the cell-specific contribution to the measured proteins. Standard biochemical analyses of enlarging tissues are usually normalized to equal amounts of global proteins loaded onto an assay (e.g. Bradford assay, immunoblotting, etc.). This standard practice, however, makes normalizing one specific protein signal to another difficult because the source of proteins in tissues may be unclear. Whole tissue preparations offer at best a “bulk sum” of all proteins from MCs, NMCs, and ECM that may mask cell-type specific changes. Single-cell analysis is preferred to limit proteome redundancy where global and/or specific proteins arise from multiple cell types or ECM[2,3].

Maturing cardiac MCs increase in size after cessation of proliferation shortly after birth and with adult specialization post-weaning[1]. While adult MCs make up a minority of cells in number, they enlarge more than 10-fold into adulthood to account for most of the adult ventricular mass[4,5]. Consideration of cell size changes is also critical when quantitating proteins. If we hypothetically load equal amounts of protein from cell lysates into a biochemical assay to compare enlarging MCs that have doubled in size and protein content, we would effectively survey half as many cells of the larger MCs as the smaller ones. An equal protein signal between samples, in fact, would not mean equal protein content per-cell, but rather that the larger MCs actually have twice as much protein as the smaller MCs. Similarly, a 50% reduction in signal on the larger MCs would mean equal protein content per-cell. This is especially problematic when changes in specific protein content or cell size occur at different rates from global proteins. Comparing developmental or diseased conditions in this scenario can potentially obscure real differences in the rate of protein accumulation or result in “false-positive” variations[6-8]. Although sarcomeres and other specialized proteins increase with cardiac mass[9], an inability to biochemically sample MC

proteins separate from NMCs and ECM contaminant can limit the validity of normalizing MC proteins to global proteins from tissues[10,11].

To overcome these challenges, we developed a highly reproducible fluorescence-activated cell-sorting (FACS) strategy that purifies known numbers of adult MCs from NMCs and ECM in single cell preparations. We have designed and optimized this new large-particle protocol (LP-FACS) using a conventional jet-in-air sorter especially fitted with a 200-μm nozzle. In this new configuration, the sorter counts and purifies adult ventricular MCs regardless of morphology. Purified MCs are then sized and used to generate protein lysates. Analyzing protein lysates from known numbers of purified and well-sized MCs permits an independent scaling of proteins of interest to global proteins (i.e. proteome) and/or myocyte growth.

To gain a new insight into the cell size-sarcomere content relationship of normally growing MCs, we purified ventricular MCs post-weaning with LP-FACS and biochemically measured MyHC and α-actin content per-cell. These two proteins are integral constituents of the sarcomere and responsible for muscle contraction. Both proteins have two isoforms differentially expressed in the heart throughout development: α & β-MyHCs[12] and α-cardiac & skeletal actins[13]. To scale the biochemical content of MC proteins to animal growth and MC sizes, we applied the simple model of ontogenic allometry[14]. This model relates the rate of change of physiological and/or molecular features to growth during development[15,16]. Using this new analytical system, we identified that sarcomeric proteins accumulate at a disproportionately higher rate than the MC-specific proteome during normal growth. Scaling specific proteins to cell size in LP-FACS purified MCs provides a new framework to understand variability in normal tissue growth at the level of individual cell types in health and disease.

BRIEF METHODS

Single-cell preparations

The Institutional Animal Care and Use Committee at the University of California, Davis, approved all animal care and procedures. C57BL/6 mice were fed standard mouse diet *ad libitum.* Mouse hearts were obtained during the postnatal period from the 1st to the 94th day of life. On postnatal day 20-21, litters were weaned and single-cell suspensions were obtained at least 1 day post-weaning. Post-weaning mice from postnatal days 21-25 were referred to as weanlings, and mice from postnatal days 75 to 94 were referred to as adults. Cardiac single-cell preparations from post-weaning mice were obtained by the methods of Lopez *et al*[10] with modifications (see supplemental methods) aimed to increase the proportion of healthy and mostly rod-shaped MCs in ventricular preparations. Briefly, coronary arteries were perfused with a nominal calcium-free perfusion buffer containing 2,3-butanedione monoxime (BDM) at 37 °C followed by collagenase enzymatic digestion and a high-K^+ HEPES containing solution at pH 7.4. This buffer sequence was optimized to yield ~85% rod-shaped MCs. To preserve the morphology of isolated adult MCs post-sorting, cells were gently fixed with 0.4% paraformaldehyde (PFA) prior to LP-FACS sorting. Neonatal and adult cell isolation followed by β-MyHC, α-MyHC, α-actin, and NPPA flow

cytometric analysis (FCM) was done on a FACScan cytometer (BD Biosciences, San Jose, CA) as previously described[10].

Adult myocyte cell sorting and analysis

LP-FACS was performed with a jet-in-air Becton Dickinson Influx Cell Sorter (BD Biosciences, San Jose, CA) modified with a 200-μm nozzle and a small particle detector upgrade on the FSC channel (threshold channel). New sort settings, single-cell preparation, cell sizing, and protein analysis methods are detailed in supplemental materials. Briefly, low-pressure settings and reduced oscillator frequency for droplet stability were developed to accommodate the larger size of adult MCs (up to ~110×40 μm) with variable fractions of cell shapes (i.e. rods vs. rounds). Cell shape is a critical factor in MC flow cytometry because it affects the propensity of large particles to align in a flow stream. Single-cell preparation, handling, and cell concentration were optimized to maximize rod-shaped MC alignment in the flow stream without excluding round MCs. Immunophenotyping with four monoclonal antibodies (mAbs) and a DNA marker provided a sort logic that can identify MCs (labeled with anti-cTnT mAb) and NMCs (labeled with CD31, CD45, and Sca-1 mAbs) independently. All primary mAbs were fluorochrome conjugated to avoid cross-contamination. Influx settings and cell labeling were designed to reach a pre-specified ≥95% MC purity (independent of morphology) with ≥90% accuracy on MC counts. The median volumes of 5,000-7,000 MCs post-sort were measured with a Coulter Multisizer 4 (Beckman Coulter, Brea, CA)[17,18].

Protein analysis

Global protein analysis using the Bradford method was performed on LP-FACS-purified MC lysates to measure MC proteome. MyHC content was determined by immunoblotting densitometry of MF-20 mAb conjugated to HRP to avoid non-specific binding and/or cross-reactivity of secondary Abs binding to primary Abs used for cell sorting. α-actin was measured similarly using 5c5 lgM mAb. Secondary anti-lgM Ab conjugated to HRP was selected to avoid cross reactivity with primary Abs used for cell sorting.”

MyHC, α-actin, and global protein signals were first standardized to cell numbers that provided a signal in linear range. The number of MCs needed for each assay was selected based on the linear range of the signal. These cell numbers were different for weanlings and adults due to ontogenic differences in cell size and protein content. Global protein content was calculated in nanograms per MC (ng/MC) for each animal. The MyHC and α-actin content per-MC in arbitrary units was normalized to the weanling samples in the same slot blot.

Ontogenic allometry and statistical analysis

Results are shown as mean±SD unless otherwise noted. Significant differences ($p<0.05$) among groups were tested in GraphPad Prism version 6.0 with 1-way ANOVA and Bonferroni multiple comparison test for more than 2 groups, or unpaired student’s *t* test for 2 groups. Protein content per-MC and MC median volumes were scaled to animal growth using the regression line between log-log covariates with the equation $y = bx^{a}$ for ontogenic allometry[15] where *y* is the trait being scaled, *x* is the growth determinant, and *b* (intercept) &

α (slope) are constants. The animal age is replaced as the growth determinant by body mass and time is cancelled out in the derivative[14,19,20]. Cell growth and protein accumulation are the traits of interest. The exponent *a* is the slope of the regression line and effectively captures the differential growth ratio between the traits and body mass as a whole[16]. This is in keeping with the power-law relationship implicit in allometric modeling. $a \approx 1$ represents a constant proportionate rate of change (but not absolute magnitude) between traits and body mass throughout ontogeny, or isometry; $\alpha > 1$ indicates that the trait has a higher growth or accumulation rate than the body as a whole, or hyperallometry; and $\alpha < 1$ indicates that the trait has a lower growth or accumulation rate than the body as a whole, or hypoallometry. The relationship among body mass and various traits were evaluated using t-tests for significant difference from a null hypothesis on α, with the associated standard error used for inference. Multiple comparisons were evaluated with a 5% false-discovery rate.

RESULTS

Ratios of age with body and heart mass in postnatal mice

Fig. 1A shows age vs. body and heart mass from postnatal days 1 to 94 mice. The correlation between both body and heart masses to age in our study cohort was high (R^2= 0.96, R^2= 0.85, respectively), but the correlation of body mass to age was closer to 1. Body mass increased 19.6 fold from neonatal day 1 (1.35±0.10 g, n=5) when compared to adults older than 75 days (26.5±1 g, n=8, p<0.0001). Heart mass increased 35.4 fold from neonatal day 1 (5.3±0.6 mg, n=5) when compared to adults older than 75 days (187.5±26 mg, n=8, p<0.0001). When comparing mean heart to body mass ratios (H/BM) in post-weaning mice, our ratios were higher than expected (8.8±2, n=16) compared to results reported by others to range from 4 to 7 mg/g[21,22]. However, neonatal mice from day 1-10 showed a H/BM ratio of 5.1 ± 1 (n=42, p<0.0001) consistent with the literature. The difference between neonatal and post-weaning H/BM ratios was unexpected and attributed to the need for preserving the aorta (i.e. extra cardiac tissue) for successful cannulations and single-cell isolations in post-weaning hearts. Given this discrepancy, we used body mass as the growth determinant for ontogenic scaling.

α- vs. β-MyHC expression in post-weaning rod-shaped MCs

At weaning, MCs are already rod shaped[23,24], the microvasculature has developed[4], and an earlier surge of thyroid hormone has contributed to α-MyHC becoming the dominant homodimer in adult mouse ventricles[12,25]. Fig. 1B shows the heterogeneity of cardiac cells (i.e. large MCs and smaller NMCs) in adult ventricular single-cell preparations. Our new and optimized buffer sequence for cell harvesting yielded $1.4\pm0.46\times10^6$ MCs (n=32) from the left ventricle (LV). It also yielded 87±11% rod-shaped MCs (n=28 harvests) in serum-free conditions. In addition, MCs had striations (Supplemental Fig. 1) and no visible surface membrane blebs which correlated with healthy MCs that exclude trypan blue[18].

To confirm the anticipated fetal switching of MyHC isoforms from β to α post-weaning, we measured the down regulation of β-MyHC, the fetal isoform, from neonates to adults. FCM analysis demonstrated lowest levels of β-MyHC (<1%) at 21-25 days (weanlings) with only a very small fraction of adult MCs (<4%) expressing the αβ-MyHC heterodimer (Fig. 1C).

Additional staining with an α-MyHC specific mAb (BA-G5) verified that this isoform is expressed in ≥95% of adult MCs but not neonates (~8%, Supplemental Fig. 2). FCM also demonstrated the reduction of NPPA, a second fetal isoform protein, which parallels β-MyHC switching (Supplemental Fig. 2).

In addition, MF20 (anti α & β–MyHC[26]) and 5c5 (anti-α-actin[13]) mAbs labeled ≥96% of all neonatal and adult MCs (Supplemental Fig. 3) independently of fetal isoform switching. Hence, our adult single-cell preparations produced a majority of healthy rod-shaped MCs (87%) that expressed mostly (>95%) α-MyHC (Fig. 1C and Supplemental Fig. 2) and α-actin[27,28] post-weaning (Supplemental Fig. 3).

Development of large particle FACS (LP-FACS) to purify adult MCs

To purify MCs for cell-specific sizing and per-cell protein analysis, we aimed to establish a new large-particle FACS protocol (LP-FACS) that could reliably isolate adult MCs independently of their morphology. Our pre-specified purity for MCs was ≥95% from an initial ventricular cell preparation where MCs start as <50% of cells and are >85% rod shaped (Fig. 1B). Using a regular FACS set-up on the BD Influx Cell Sorter, a jet-in-air system fitted with a standard 100-μm nozzle, preliminary attempts failed at reaching our targeted purity level. This system repeatedly failed at generating a hydrodynamically aligned stream of large rod-shaped MCs. As previously described by others, it yielded mostly damaged MCs[29] or a clogged instrument[17]. To overcome these limitations, we redefine the set up to accommodate a nozzle tip of 200-μm for a large-particle sort. Optimal settings and sample preparations had to be empirically defined (as detailed in the supplement). The new settings had to stabilize the fluidic stream at lower driving pressures and give rise to a stable production of droplets above the point of entry into the electrostatic field responsible for droplet deflection[30]. The flow frequency that provided a stable breakoff distance of 280-300 units optimal for larger adult rod-shaped MC sorting was 6.48 kHz @ 3.7 psi.

New sort logic independent of cell-size and side-scatter

The sort purity also depends on the sort logic. Supplemental Fig. 4 shows the inadequacy of a light-scatter size-based sort logic to reach the benchmarked purity with the LP-FACS set up. This inadequacy was due to poor sorter sensitivity in identifying the coincidence of large MCs and smaller NMCs present in a single droplet targeted for purification. This unwanted random occurrence does not allow the sorter to abort these “contaminated” drops from being dispensed into the purified population. A new sort logic, shown in Fig. 2A, was then tested to inform the sort algorithm to abort these drops from the collection. This new approach combined a 2-drops, purity mode with 8-coincidence logic with a negative selection step to abort contaminated large drops. A contaminated drop was identified by a nucleated cell signal expressing cell-surface markers for any one of multiple NMCs (CD31, CD45 and Sca-1) known to be present in muscle preparations[10,31,32]. A targeted drop was defined as a NMC-negative nucleated cell that labeled positively for cardiac Troponin T (cTnT), a sarcomeric regulatory protein only expressed in MCs. Using this 3-step immunophenotyped logic, adult LV MC isolations reached 95+2% purity while RV MCs reached 93±1% (Fig. 2B). Taken together, we required a negative NMC and positive MC labeling to generate ±95% MC purity.

LP-FACS benchmarks when sorting large cardiac MCs

Sorted adult and weanling MCs remained mostly rod-shaped post-sort (85±9%, *p*=ns vs. pre-sort, n=10, Fig. 1B and 2C). Accuracy in sorted MC counts is required to normalize protein content per-MC in biochemical assays. This was tested in triplicate with every sort as a quality control step. Fig. 2C also shows a count accuracy of 92±1% (n=19) between runs and with a coefficient of variation <5% within a run for both ventricles. This level of precision and accuracy is above what is previously reported in standard cell sorters[33] and demonstrates the success of our LP-FACS method to purify adult MCs for downstream analysis with accurate counting and without altering morphology.

Cell sizing of LP-FA CS sorted MCs

The mean length of sorted adult LV MCs (109.2±7.1 μm, 100 cells counted from 5 LVs) was 21% longer (*p*=0.065) than the weanlings (90.0±14μm, 100 cells counted from 8 LVs). The mean width of sorted adult LV MCs (32.4±6.5μm) was 26% wider (*p*=0.065) than the weanlings (25.8±2.2μm). To rapidly size MC post-sort, we utilized a Coulter Multisizer. This technology is a robust and validated assay that accurately measures cell volumes of rod and round-shaped MCs independently of shape[18,34]. We analyzed 5,000-7,000 LP-FACS sorted LV MCs as shown in Fig. 3A. The median volume of adult MCs (33,458±8,251 μm^3, n=7) was 275% larger (*p*<0.0001) than weanlings (12,176±4,008μm^3, n=8). Given the robustness of the MC volume measurement, we utilized this size trait for ontogenic scaling.

Scaling of LV MC volume and body mass in post-weaning mice

To scale the rate of growth of LV MCs post-weaning, we plotted the median volumes of purified MCs vs. body mass in a log-log transformed plot as shown in Fig. 3B. The resultant linear equation is $y=1128\times^{1.02}$ where the coefficient α is 1.02, and not significantly different from 1 (*p*=0.87, 95% CI = 0.76 to 1.28). This indicated that there is no difference in growth rates between MC volumes and body mass. Although the absolute values of both traits increased by ~275%, they maintained isometry that is consistent with a proportionate ratio of growth.

MC proteome and sarcomeric proteins quantification per-cell in post-weaning LV MCs

To scale the rate of accumulation of the MC proteome and sarcomeric proteins per MC, we purified 10,000 MCs with LP-FACS and prepared protein lysates for biochemical analysis. Careful protocol design assured that cell purity (Fig. 2B), counts and morphology (Fig. 2C), lysates, and cell volumes (Fig. 3) obtained from separate sort runs (always done on the same day) were comparable to one another. Fig. 4A & B show sample slot blots of LP-FACS purified MCs from three weanlings and three adult LVs immunoblotted for MyHC and α-actin respectively. Due to the absence of a protein separation step to distinguish isoforms, we assayed α-MyHC content with MF-20 mAb and α-actin content with 5c5 mAb. Both mAbs are highly specific for both isoforms of sarcomeric proteins independently of fetal switching (Supplemental Fig 3) in striated muscle[13,26].

To evaluate the precision and linearity of immunoblotting, different MC numbers were loaded from weanlings and adults. The ranges of loaded cell numbers for each protein were empirically selected to fall in a linear range of densitometry signal (Supplemental Fig. 5).

The correlation coefficients within groups of samples were excellent (R^2 ranged from 0.97 to 0.71). From each densitometry band, the sarcomeric protein signal in arbitrary units per-MC was calculated (NIH Image), averaged, and normalized to the average value from weanlings in the same blot. The MyHC (Fig. 4A) and α-actin (Fig. 4B) content from immunoblots were analyzed similarly. Per-MC proteome was calculated similarly to sarcomeric proteins by dividing the global protein content in nanograms by the number of purified MCs in the lysate.

Growth scaling of proteome and sarcomeric proteins accumulation post-weaning

The content of MC proteome (ng/MC) in post-weaning LV MCs was plotted vs. body mass in log-log transformed plots as shown in Fig. 4C (left panel). The rate of MC proteome accumulation was derived from the equation $y=0.15\times^{0.94}$ where the coefficient α is 0.94. This was not significantly different from 1 (p=0.76, 95% CI = 0.47 to 1.41). This isometric coefficient was identical to that of MC proteome vs. MC volumes (α = 0.96, p = 0.85, CI = 0.42 to 1.49).

The normalized density of α-MyHC per-MC was then plotted vs. body mass. The rate of α-MyHC accumulation is derived from the equation $y=0.02\times^{1.79}$ where the coefficient α is 1.79 and significantly higher from 1 (p=0.0037, 95% CI = 1.37 to 2.31). This hyperallometric coefficient also characterized the accumulation α-MyHC when plotted vs. MC volumes (α = 1.76, p = 0.051, CI = 0.99 to 2.53). The normalized density of α-actin per-MC was also plotted vs. body mass. The rate of α-actin accumulation is derived from the equation $y=0.006\times^{2.18}$ where the coefficient α is 2.18 and significantly higher from 1 ($p<0.0001$, 95% CI = 2.12 to 2.24). This hyperallometric coefficient also characterized the accumulation of α-actin when plotted vs. MC volumes (α = 1.45, p = 0.041, CI = 1.07 to 1.83). A summary model in Fig. 4C (right panel) depicts an overlay of the hyperallometric scales of α-MyHC and α-actin as compared to the proportional MC volumes and accumulation of the proteome when scaled to body mass.

DISCUSSION

To allocate protein changes to a specific cell-type, we developed and validated a LP-FACS-based approach to purify MCs and NMCs from a heterogeneous adult ventricular preparation using a new large-particle cell sorting system. The main accomplishment of this study is the reliable isolation of up to 10,000 ventricular MCs with ≥95% purity using cell-type specific immunophenotyping. This approach isolates MCs from NMCs and ECM to measure the MC sizes and generate pure MC lysates for biochemical analysis of cellular proteins per-cell. Protein assays were normalized to MC-specific numbers. This circumvents normalizing cell-type specific proteins to global proteins in heterogeneous tissues or enlarging cells. Per-cell normalization does not assume that cell size and protein accumulation are always proportional or dependent on one another. As seen in Fig. 3 and 4, these measurements are treated in our analyses as independent outcomes and permit independent scaling of molecular traits to morphological measurement.

To test our new system, we measured the biochemical correlation of two sarcomeric proteins and the MC proteome to cell size and body mass during normal post-weaning growth. This

study biochemically quantitates, for the first time, the disproportionate growth scale of sarcomeric proteins to the MC proteome. This finding suggests the existence of separate mechanisms for regulating these in relation to cell size. Our approach integrates innovations in three distinctive areas: 1) optimization of single cell isolations of rod-shaped MCs from adult ventricles; 2) development of a large-particle FACS sorting strategy to purify adult MCs; and 3) the application of allometric modeling to scale biochemically assayed proteins per-cell to body and MC growth. This single-MC analysis provides a foundation for studying the variability in normal tissue proteostasis at the level of individual cells. More importantly, this approach provides a valuable tool to quantitating any other cell-type specific protein, DNA, or RNA molecules from cells of variable sizes with per-cell normalization.

Optimization of adult single cell isolations for per-MC analysis

At the core of single-cell analysis is the principle that purified cell populations post-sorting represent the original parent population obtained from a heterogeneous mix. For this study, we modified our prior enzymatic single-cell dispersion of ventricular cells[10,24] with a new buffer sequence. This new protocol doubled the fraction of rod-shaped MCs in suspension to >85% as compared to our previous report (43%)[10], and provided an improvement from that of others[23,24,29,35]. This improvement is attributed to three factors in the digestion/dispersion buffers: 1) the presence of BDM that blocks myosin ATPase and inhibits spontaneous contractions[24]; 2) the elimination of serum to block protease after digestion; and 3) the use of supra-physiological potassium buffer for the diastolic arrest of MCs at the time of dissociation. Early trials sorting live MCs, however, yielded dysmorphic MCs that precluded reliable morphologic measurements of MC health post-sort. Hence, a low-concentration of PFA for cell fixation was used to preserve MC morphology in the preparation. PFA was preferred because, unlike ethanol[36], it does not shrink cells[37]. After fixation, all cell centrifugations, wash steps, and sort algorithms were carefully optimized to overcome NMC and ECM contamination. More importantly, we monitored and validated that these steps did not disrupt the morphology of the healthy rod-shaped MCs obtained in the parent population.

Large-particle FACS sorting of adult cardiac myocytes

We utilized a jet-in-air sorter fitted for the first time with a 200-μm nozzle and defined new settings to isolate from the smallest cells (i.e. NMCs) to the largest (i.e. rod-shaped MCs). Under normal hydrodynamic conditions, the cell stream in the sorter is optimally focused down to <1/5 of the nozzle size. In the case of our oldest adult MCs that measured up to ~110×40 μm, the MC diameter to the 200-μm nozzle ratio would be optimal at ~1/5 if the largest MCs align along their long axis in the stream. This set up overcame the biophysical challenges of standard sorter with smaller nozzles to isolate the larger rod-shaped MCs from adult hearts[29,38]. Cell alignment in the focused stream is imperative for a successful sort and to minimize instrument clogging.

Avoidance of particle coincidence (i.e. two or more particles in a single drop) is also important to generate pure drops in air for sorting. A low MC concentration in suspension is critical to align the long axis of rod-shaped MCs with the flow direction and minimizes the

coincidence of more than two MCs flowing together and clogging the instruments[10,17]. A major biophysical challenge using a 200-μm nozzle with low cell concentration in suspension is maintaining a stable fluid pressure and stable flow stream. Our careful balance of cell concentration, flow rate, and driving pressure was critical to generate sort droplets at a stable break off distance. Since these settings turned out to be cell morphology dependent, the optimal set up had to be empirically defined in the Influx sorter using targeted cells and then validated by light microscopy, FCM, and cell counting post-FACS (Fig. 1B and 2B,C).

Immunophenotyping of adult cardiac myocytes for LP-FACS sorting

Using cell size and light-scatter parameters in the sort logic as previously reported in standard sorters[29,38] only achieved ~85% MC purity in the 200-μm set up (Supplemental Fig. 4). This was largely due to a propensity for rod-shaped MCs, the majority of MCs in the post-weaning preparations, and NMCs to coincide in a single drop. In our final algorithm, the combination of a nucleated cell gate with both NMC-negative and MC-positive ($cTnT^+$) gates were required to reach the pre-specified ≥95% benchmark of MC purity. A downside of labeling MCs with cTnT mAb for sorting is that this protein cannot be used for immunoblotting, as this epitope may be pre-blocked with the FCM mAb present in the lysate. By reducing NMC contaminants to <5% with our algorithm, MC lysates from sorted cells can be considered a pure MC sample for protein analysis. LP-FACS performed well when isolating NMCs (Supplemental Fig. 4) that are usually round and <30μm. This establishes the robustness of this new set-up to purify cardiac cells from a broad spectrum of sizes and morphology present in the adult heart.

Allometric modeling for scaling proteins

In ontogenic allometry, a trait of interest (i.e. cell size or protein content) can be scaled to a growth determinant (i.e. body mass) in a single species as it grows from zygote into adulthood[15,39]". Using the linear regression equation of the log-log transform plot for the trait of interest and growth determinant, the a coefficient (exponent) is the slope of the regression line. This dimensionless coefficient represents the rate of protein accumulation as a function of growth. This type of modeling is a preferred alternative to ratiometric methods because assumptions about units and/or variance between traits are usually not needed[40]. Our data show proportional (i.e. isometric) growth between body mass and MC volumes that is consistent with prior morphometric analyses in the post-weaning period[4,19]. This animal-to-cell isometry occurred while MCs grew by 275% in volume. Since our analysis of sorted MC growth yielded consistent results with prior morphometric studies, we moved ahead with the ontogenic scaling of assayed proteins in isolated single cells.

Isometric growth scaling of MC proteome post-weaning

In the prenatal heart, MCs proliferate and waves of cell migration contribute to cardiac mass and morphogenesis[41]. Shortly after birth, MCs cease cell division with a last round of DNA replication without cytokinesis[1]. Although the exact timing of this cessation is controversial[22,42,43], it is agreed that MC proliferation is over by weaning in rodents[8,21,22,44]. Post-weaning is the first time that cardiac mass increases solely by an increase in MC size and accumulation of sarcomeres per MC to meet the demands of physical activity into adulthood[5,45]. Hence, we scaled biochemically the rate of protein

accumulation to body mass and MC volume in post-weaning, non-proliferating MCs that grow only in size. Our analysis shows that the rate of MC proteome accumulation is isometric to body and MC growth (α=0.94 and 0.97, respectively). This suggested that a MC size-proteome sensing feedback may exist in these non-proliferating MCs to maintain this isometry[46].

Hyperallometric growth scaling of sarcomeric proteins in ontogeny

The isometric growth scale of the MC proteome is in stark contrast to the divergence of α-MyHC and α-actin accumulation in this period of ontogeny. Our results indicate that α-MyHC protein accumulates at a much greater rate than body mass (α=1.79) and MC volumes (α=1.76). In parallel, α-actin accumulates at a much greater rate than body mass (α=2.18) and MC volumes (α=1.45). These results support that this sarcometric protein accumulation is coordinated and beyond what is predicted by the increase of the MC proteome or size during this ontogenic period. Presumably, this positive rate of accumulation can be considered biochemical evidence of muscle specialization. A sarcomeric protein accumulation that scales above cell size likely provides additional contractility when mice are more physically active seeking food on their own. While multiple studies have observed an isometric accumulation of cardiac ultrastructure (i.e. myofibers) by evaluating the %-volume density in tissue images, none have biochemically measured before these proteins per-MC.

MyHC Hyperallometric growth scaling in pathological hypertrophy

The ontogenic hyperallometry of MyHC in this study is in contrast to previously published data on a-MyHC expressing MCs in the trans aortic constriction model (TAC). The pressure-overloaded MCs that express α-MyHC (~75% of MCs) in this model accounted for most of the hypertrophy (HT) but had relatively less MyHC mRNA[47] and protein[10] than predicted by cardiac mass or MC size respectively. Using fluorescence data presented in Online Figure III from the study by Lopez et al.[10], the a coefficient for MyHC in these MCs was estimated at ~0.53 or hypoallometric. In contrast, the β-MyHC expressing MCs (~25% of MCs) that minimally HT (<10%) in this model increased their MyHC content by 41%. Their α coefficient was estimated at ~3.6 or hyperallometric. We proposed that the MyHC hypoallometry in α-MyHC expressing MCs after TAC is part of a maladaptive phenotype given the additional hemodynamic load placed on these MCs. Meanwhile, the hyperallometry of β-MyHC expressing MCs appeared more adaptive because of additional MyHC content to handle the additional load. This type of MCs growth after TAC was previously described as normotrophy[11] and is on par with the hyperallometry of normal α-MyHC expressing MCs found in the current study. We propose that the term normotrophy can be used broadly to describe enlarging MCs with sarcomeric protein hyperallometry since we have now shown that this process is not restricted to disease or development alone.

Limitations

The use of fixed cells, which precludes studying native proteins in physiological environments or MC culturing is a limiting factor in our study. Further technological advancements will be needed to study live adult MCs post-sorting in these jet-in-air systems since we observed cell breakage that reduces viability. Furthermore, only male mice were

sampled in this study due to the known substantial differences between males and females in growth curves post-weaning[48,49]. Future studies will need to explore if sex variants exist between MC growth and protein content. Additionally, the cellular/molecular mechanisms coordinating higher concentrations of sarcomeric proteins in relation to MC size and an isometric proteome during MC ontogenic growth are not addressed in this study.

Future directions

How a normal or diseased MC differentially regulates its global proteome and sarcomeric protein content during cell growth is presently unknown. Normalizing protein content to MC numbers and/or types should maximize the confidence that future proteomic analysis in cardiac growth is representative of variable MCs changes in size. LP-FACS purified MCs also offer a new entry point for cell-specific analysis into relationship between cellular organization and function, as well as variations in normal cardiac tissues[50] at the level of individual cells.

With new resolution into cell-type specific purifications and cell-to-cell variations, a future search for cell size sensors responsive to normal cardiac growth or normotrophy is within reach. These sensors are described in other systems[46,51] and likely consists of the integration of cell-autonomous (i.e. cell-size check point(s)), non-cell-autonomous (i.e. nutrition, extracellular growth factors, mechanical stress, ECM[51-54]) and/or ligand-receptors interactions (e.g. thyroid hormone[43], insulin-like receptors[55,56], adrenergic receptors[57], etc.) as previously identified in cardiac hypertrophy. Reports on the cell-to-cell imbalances in gene expression[8], heterogeneous expression of sarcomeric proteins[10,47,58,59], and adrenergic receptors[60] in cardiac cell sub-populations underscore the application of LP-FACS purifications to assay the functional implications of individual cell variations.

Beyond these factors, MCs need to coordinate differential levels of protein synthesis, folding, and turnover to concentrate sarcomeric proteins and maintain normal proteostasis[61,62]. Future growth scaling of these cellular processes in MCs of variable sizes and/or function should also provide new insight into cell-size-sarcomere regulators of contractility[8,10,63]. More broadly, our validated LP-FACS approach provides a framework for future scaling of multiple cellular and molecular processes in MCs of variable sizes already known to exist in a single heart preparation[64,65].

Supplementary Material

Refer to Web version on PubMed Central for supplementary material.

Acknowledgments

The authors would like to thank Shadi Aminololama-Shakeri, M.D., Ms. Elaje A. López and Ms. Diana Angelica Ramos for their critical review of the manuscript.

SOURCES OF FUNDING

This study was supported in part by the Harold Amos Medical Faculty Development Program from the Robert Wood Johnson Foundation (J.E.L.), Western States Affiliate of the American Heart Association Beginning Grant-in-Aid (J.E.L), the Department of Veterans Affairs and the NIH (P.C.S.HL31113, N.C.-NIH R01 HL085844, NIH R01 HL085727, NIH R01 HL137228 and VA I01 BX000576), the National Center for Advancing Translational

Sciences, NIH, grant number UL1 TR001860 and linked award KL2 TR001859 (J.E.L.). N.C. is the holder of the Roger Tatarian Endowed Professor in Cardiovascular Medicine

Non-standard Abbreviations

Ab	antibody
α-actin	alpha-actin
APC	allophycocyanin
BDM- 2	3-butanedione monoxime
cTnT	cardiac troponin T
DAPI	4′, 6-diamidino-2-phenylindole
DSHB	Developmental Studies Hybridoma Bank
ECM	extra cellular matrix
FCM	Flow cytometric analysis
H/BM	heart to body mass ratio
HRP	horseradish peroxidase
HT	hypertrophy
LP-FACS	large-particle fluorescent-activated cell sorting
mAb	monoclonal antibody MC, myocyte
MF20	anti-myosin heavy chain monoclonal antibody
MyHC	myosin heavy chain
NMC	non-muscle cell
PI	propidium iodide
PFA	paraformaldehyde

References

1. Bugaisky L, Zak R. Cellular growth of cardiac muscle after birth. Tex Rep Biol Med. 1979; 39:123–138. [PubMed: 162244]
2. Wu M, Singh AK. Single-cell protein analysis. Current opinion in biotechnology. 2012; 23:83–88. [PubMed: 22189001]
3. Agnetti G, Husberg C, Van Eyk JE. Divide and conquer: the application of organelle proteomics to heart failure. Circ Res. 2011; 108:512–526. [PubMed: 21335433]
4. Korecky B, Rakusan K. Normal and hypertrophic growth of the rat heart: changes in cell dimensions and number. Am J Physiol. 1978; 234:H123–128. [PubMed: 146437]
5. Anversa P, Ricci R, Olivetti G. Quantitative structural analysis of the myocardium during physiologic growth and induced cardiac hypertrophy: a review. J Am Coll Cardiol. 1986; 7:1140–1149. [PubMed: 2937828]

6. Ferguson RE, Carroll HP, Harris A, et al. Housekeeping proteins: a preliminary study illustrating some limitations as useful references in protein expression studies. Proteomics. 2005; 5:566–571. [PubMed: 15627964]
7. Ma C, Fan R, Ahmad H, et al. A clinical microchip for evaluation of single immune cells reveals high functional heterogeneity in phenotypically similar T cells. Nat Med. 2011; 17:738–743. [PubMed: 21602800]
8. Kraft T, Montag J, Radocaj A, et al. Hypertrophic Cardiomyopathy: Cell-to-Cell Imbalance in Gene Expression and Contraction Force as Trigger for Disease Phenotype Development. Circ Res. 2016; 119:992–995. [PubMed: 27737944]
9. Olivetti G, Anversa P, Loud AV. Morphometric study of early postnatal development in the left and right ventricular myocardium of the rat. II. Tissue composition, capillary growth, and sarcoplasmic alterations. Circ Res. 1980; 46:503–512. [PubMed: 6444555]
10. Lopez JE, Myagmar BE, Swigart PM, et al. beta-myosin heavy chain is induced by pressure overload in a minor subpopulation of smaller mouse cardiac myocytes. Circ Res. 2011; 109:629–638. [PubMed: 21778428]
11. Pandya K, Smithies O. beta-MyHC and cardiac hypertrophy: size does matter. Circulation Research. 2011; 109:609–610. [PubMed: 21885833]
12. Ng WA, Grupp IL, Subramaniam A, et al. Cardiac myosin heavy chain mRNA expression and myocardial function in the mouse heart. Circ Res. 1991; 68:1742–1750. [PubMed: 2036722]
13. Skalli O, Gabbiani G, Babai F, et al. Intermediate filament proteins and actin isoforms as markers for soft tissue tumor differentiation and origin. II. Rhabdomyosarcomas. Am J Pathol. 1988; 130:515–531. [PubMed: 3279794]
14. Rakusan K, Korecky B, Roth Z, et al. Development of the Ventricular Weight of the Rat Heart with Special Reference to the Early Phases of Postnatal Ontogenesis. Physiol Bohemoslov. 1963; 12:518–525. [PubMed: 14097871]
15. Huxefy JS, Jeissilr G. Terminology and notation in the description of the relative growth. Cr Soc Biol. 1936; 121:934–937.
16. Shingleton A. The Study of Biological Scaling. Nature Education Knowledge. Nature Education Knowledge. 2010; 3:6.
17. Nash GB, Tatham PER, Powell T, et al. Size Measurements on Isolated Rat-Heart Cells Using Coulter Analysis and Light Scatter Flow Cytometry. Biochimica Et Biophysica Acta. 1979; 587:99–111. [PubMed: 114233]
18. Gerdes AM, Moore JA, Hines JM, et al. Regional differences in myocyte size in normal rat heart. Anat Rec. 1986; 215:420–426. [PubMed: 3740478]
19. Mattfeldt T, Mall G. Growth of capillaries and myocardial cells in the normal rat heart. J Mol Cell Cardiol. 1987; 19:1237–1246. [PubMed: 2965252]
20. Snelling EP, Taggart DA, Maloney SK, et al. Scaling of left ventricle cardiomyocyte ultrastructure across development in the kangaroo Macropus fuliginosus. J Exp Biol. 2015; 218:1767–1776. [PubMed: 25908057]
21. Soonpaa MH, Kim KK, Pajak L, et al. Cardiomyocyte DNA synthesis and binucleation during murine development. Am J Physiol. 1996; 271:H2183–2189. [PubMed: 8945939]
22. Naqvi N, Li M, Calvert JW, et al. A proliferative burst during preadolescence establishes the final cardiomyocyte number. Cell. 2014; 157:795–807. [PubMed: 24813607]
23. Hilal-Dandan R, Kanter JR, Brunton LL. Characterization of G-protein signaling in ventricular myocytes from the adult mouse heart: differences from the rat. J Mol Cell Cardiol. 2000; 32:1211–1221. [PubMed: 10860764]
24. O'Connell TD, Rodrigo MC, Simpson PC. Isolation and culture of adult mouse cardiac myocytes. Methods Mol Biol. 2007; 357:271–296. [PubMed: 17172694]
25. Izumo S, Lompre AM, Matsuoka R, et al. Myosin heavy chain messenger RNA and protein isoform transitions during cardiac hypertrophy. Interaction between hemodynamic and thyroid hormone-induced signals. J Clin Invest. 1987; 79:970–977. [PubMed: 2950137]
26. Bader D, Masaki T, Fischman DA. Immunochemical analysis of myosin heavy chain during avian myogenesis in vivo and in vitro. J Cell Biol. 1982; 95:763–770. [PubMed: 6185504]

27. Mayer Y, Czosnek H, Zeelon PE, et al. Expression of the genes coding for the skeletal muscle and cardiac actions in the heart. Nucleic Acids Res. 1984; 12:1087–1100. [PubMed: 6546444]
28. Tondeleir D, Vandamme D, Vandekerckhove J, et al. Actin isoform expression patterns during mammalian development and in pathology: insights from mouse models. Cell Motil Cytoskeleton. 2009; 66:798–815. [PubMed: 19296487]
29. Diez C, Simm A. Gene expression in rod shaped cardiac myocytes, sorted by flow cytometry. Cardiovasc Res. 1998; 40:530–537. [PubMed: 10070494]
30. Galbraith, DW., Lucretti, S. Large Particle Sorting. In: Radbruch, A., editor. Flow Cytometry and Cell Sorting. Berlin, Heidelberg: Springer Berlin Heidelberg; 2000. p. 293-317.
31. Pinto AR, Ilinykh A, Ivey MJ, et al. Revisiting Cardiac Cellular Composition. Circ Res. 2016; 118:400–409. [PubMed: 26635390]
32. Lopez JE, Epting CL, Pedersen A, et al. Stem cell antigen-1 regulates the tempo of muscle repair through effects on proliferation of alpha7 integrin-expressing myoblasts. Exp Cell Res. 2008; 314:1125–1135. [PubMed: 18073129]
33. Alberti S, Stovel R, Herzenberg LA. Preservation of cells sorted individually onto microscope slides with a fluorescence-activated cell sorter. Cytometry. 1984; 5:644–647. [PubMed: 6518940]
34. Campbell SE, Korecky B, Rakusan K. Remodeling of myocyte dimensions in hypertrophic and atrophic rat hearts. Circ Res. 1991; 68:984–996. [PubMed: 1826234]
35. Ackers-Johnson M, Li PY, Holmes AP, et al. A Simplified, Langendorff-Free Method for Concomitant Isolation of Viable Cardiac Myocytes and Nonmyocytes From the Adult Mouse Heart. Circ Res. 2016; 119:909–920. [PubMed: 27502479]
36. Chao Y, Zhang T. Optimization of fixation methods for observation of bacterial cell morphology and surface ultrastructures by atomic force microscopy. Appl Microbiol Biotechnol. 2011; 92:381–392. [PubMed: 21881891]
37. Fox CH, Johnson FB, Whiting J, et al. Formaldehyde fixation. J Histochem Cytochem. 1985; 33:845–853. [PubMed: 3894502]
38. Malliaras K, Zhang Y, Seinfeld J, et al. Cardiomyocyte proliferation and progenitor cell recruitment underlie therapeutic regeneration after myocardial infarction in the adult mouse heart. EMBO molecular medicine. 2013; 5:191–209. [PubMed: 23255322]
39. Klingenberg CP. Studying morphological integration and modularity at multiple levels: concepts and analysis. Philos Trans R Soc Lond B Biol Sci. 2014; 369:20130249. [PubMed: 25002695]
40. Dewey FE, Rosenthal D, Murphy DJ Jr, et al. Does size matter? Clinical applications of scaling cardiac size and function for body size. Circulation. 2008; 117:2279–2287. [PubMed: 18443249]
41. Srivastava D, Olson EN. Knowing in your heart what's right. Trends Cell Biol. 1997; 7:447–453. [PubMed: 17709004]
42. Hirai M, Chen J, Evans SM. Tissue-Specific Cell Cycle Indicator Reveals Unexpected Findings for Cardiac Myocyte Proliferation. Circ Res. 2016; 118:20–28. [PubMed: 26472817]
43. Zhang CH, Kuhn B. Muscling up the heart: a preadolescent cardiomyocyte proliferation contributes to heart growth. Circ Res. 2014; 115:690–692. [PubMed: 25258401]
44. Walsh S, Ponten A, Fleischmann BK, et al. Cardiomyocyte cell cycle control and growth estimation in vivo–an analysis based on cardiomyocyte nuclei. Cardiovasc Res. 2010; 86:365–373. [PubMed: 20071355]
45. Li F, Wang X, Capasso JM, et al. Rapid transition of cardiac myocytes from hyperplasia to hypertrophy during postnatal development. J Mol Cell Cardiol. 1996; 28:1737–1746. [PubMed: 8877783]
46. Leslie M. How Does a Cell Know Its Size? Science. 2011; 334:1047–1048. [PubMed: 22116854]
47. Pandya K, Cowhig J, Brackhan J, et al. Discordant on/off switching of gene expression in myocytes during cardiac hypertrophy in vivo. Proc Natl Acad Sci U S A. 2008; 105:13063–13068. [PubMed: 18755891]
48. BODY WEIGHT INFORMATION FOR C57BL/6J (000664). https://wwwjaxorg/jax-mice-and-services/strain-data-sheet-pages/body-weight-chart-000664.

49. Yang Y, Smith DL Jr, Keating KD, et al. Variations in body weight, food intake and body composition after long-term high-fat diet feeding in C57BL/6J mice. Obesity. 2014; 22:2147–2155. [PubMed: 24942674]
50. Chang CW, Dalgliesh AJ, Lopez JE, et al. Cardiac extracellular matrix proteomics: Challenges, techniques, and clinical implications. Proteomics Clin Appl. 2016; 10:39–50. [PubMed: 26200932]
51. Jorgensen P, Tyers M. How cells coordinate growth and division. Curr Biol. 2004; 14:R1014–1027. [PubMed: 15589139]
52. Olson EN, Schneider MD. Sizing up the heart: development redux in disease. Genes Dev. 2003; 17:1937–1956. [PubMed: 12893779]
53. Machackova J, Barta J, Dhalla NS. Myofibrillar remodeling in cardiac hypertrophy, heart failure and cardiomyopathies. Can J Cardiol. 2006; 22:953–968. [PubMed: 16971981]
54. Mall G, Mattfeldt T, Mobius HJ, et al. Stereological study on the rat heart in chronic alimentary thiamine deficiency–absence of myocardial changes despite starvation. J Mol Cell Cardiol. 1986; 18:635–643. [PubMed: 3735443]
55. Wang KC, Botting KJ, Padhee M, et al. Early origins of heart disease: low birth weight and the role of the insulin-like growth factor system in cardiac hypertrophy. Clin Exp Pharmacol Physiol. 2012; 39:958–964. [PubMed: 22774980]
56. Porrello ER, Widdop RE, Delbridge LM. Early origins of cardiac hypertrophy: does cardiomyocyte attrition programme for pathological ‘catch-up’ growth of the heart? Clin Exp Pharmacol Physiol. 2008; 35:1358–1364. [PubMed: 18759854]
57. O’Connell TD, Jensen BC, Baker AJ, et al. Cardiac alpha1-adrenergic receptors: novel aspects of expression, signaling mechanisms, physiologic function, and clinical importance. Pharmacol Rev. 2014; 66:308–333. [PubMed: 24368739]
58. Pandya K, Kim HS, Smithies O. Fibrosis, not cell size, delineates beta-myosin heavy chain reexpression during cardiac hypertrophy and normal aging in vivo. Proc Natl Acad Sci U S A. 2006; 103:16864–16869. [PubMed: 17068123]
59. Schiaffino S, Samuel JL, Sassoon D, et al. Nonsynchronous accumulation of alpha-skeletal actin and beta-myosin heavy chain mRNAs during early stages of pressure-overload–induced cardiac hypertrophy demonstrated by in situ hybridization. Circ Res. 1989; 64:937–948. [PubMed: 2523262]
60. Myagmar BE, Flynn JM, Cowley PM, et al. Adrenergic Receptors in Individual Ventricular Myocytes: The Beta-1 and Alpha-1B Are in All Cells, the Alpha-1A Is in a Subpopulation, and the Beta-2 and Beta-3 Are Mostly Absent. Circ Res. 2017; 120:1103–1115. [PubMed: 28219977]
61. Willis MS, Patterson C. Proteotoxicity and cardiac dysfunction–Alzheimer’s disease of the heart? N Engl J Med. 2013; 368:455–464. [PubMed: 23363499]
62. McLendon PM, Robbins J. Proteotoxicity and cardiac dysfunction. Circ Res. 2015; 116:1863–1882. [PubMed: 25999425]
63. Rice R, Guinto P, Dowell-Martino C, et al. Cardiac myosin heavy chain isoform exchange alters the phenotype of cTnT-related cardiomyopathies in mouse hearts. J Mol Cell Cardiol. 2010; 48:979–988. [PubMed: 20004663]
64. Chen X, Wilson RM, Kubo H, et al. Adolescent feline heart contains a population of small, proliferative ventricular myocytes with immature physiological properties. Circ Res. 2007; 100:536–544. [PubMed: 17272809]
65. Rota M, Hosoda T, De Angelis A, et al. The young mouse heart is composed of myocytes heterogeneous in age and function. Circ Res. 2007; 101:387–399. [PubMed: 17601802]

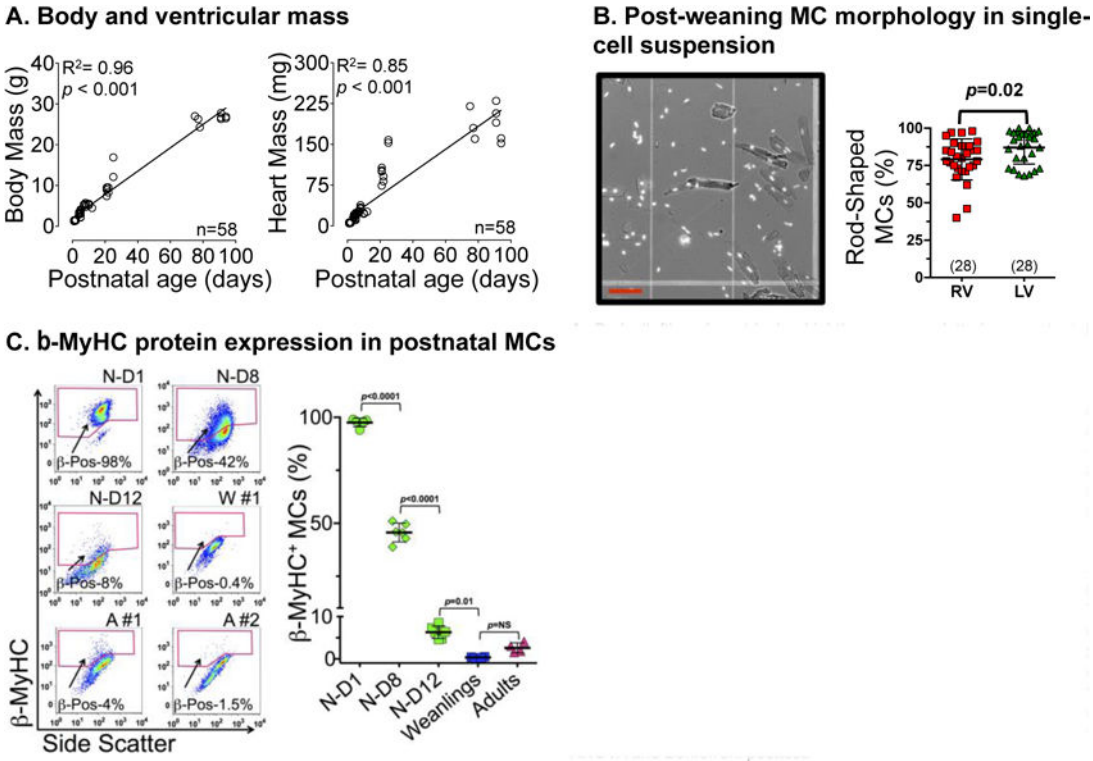

Figure 1. Postnatal growth and b-MyHC expression in rod-shaped MCs

A, Body (left) and ventricular (right) mass are plotted vs. postnatal age. R^2 is calculated by linear regression.

B, Single cells isolated from an adult left ventricle (LV) were fixed, and the fraction of rod-shaped ventricular MCs was counted in a hemocytometer. On the left panel, cellular DNA is labeled with propidium iodide (PI) to identify cell nuclei. Note the ~2:1 ratio of non-muscle small cells to MCs. Red scale bar denotes 100 μm. Values are mean±SD from right ventricle (RV, red squares) and LV (green triangles), *p* is calculated by Student t test. Number of ventricles is in parentheses.

C, Ventricular cells isolated from neonatal day 1, 8 and 12 (green, N-D1, D8, and D12 respectively), weanlings (blue, W #1), and adult (red A #1-2) mice were stained with PI to gate nucleated cells, anti-cTnT mAb to gate on MCs, and NOQ7.5.4D mAb to identify the expression of b-MyHC isoform (pink gates). Bivariate flow cytometry plots depict 5,000-10,000 MCs per heart. Background signal is defined by isotype Ab in the same MC population and used to set the pink gate for positive MCs within each developmental time point. Values are mean±SD values from four ventricles per group. *p* is calculated by 1-way ANOVA and Bonferroni posttest.

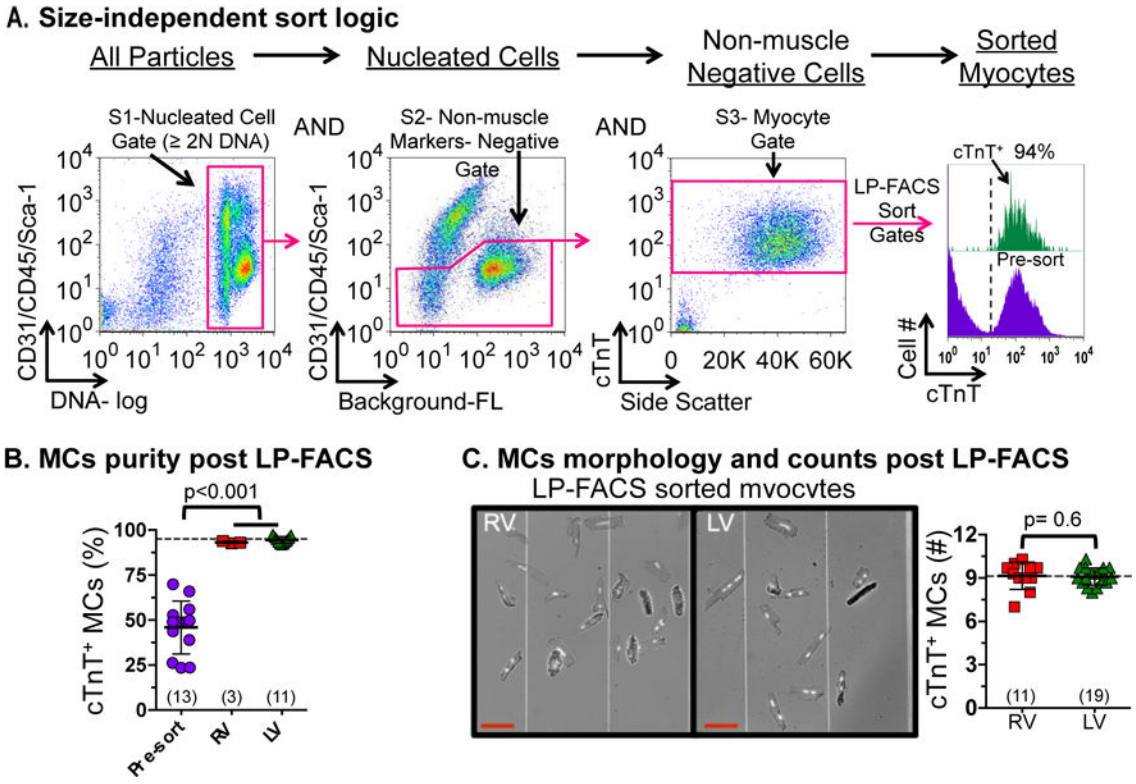

Figure 2. Adult MC purification by cell-type specific immunophenotyping and LP-FACS

A, Single cell suspensions were prepared as shown in figure 1. A new size-independent sort logic based on immunophenotyping is shown in 3 steps. In step 1 (S1), the DNA content of cells is labeled with DAPI to gate for nucleated cells (pink gate). In step 2 (S2), nucleated cells are gated out if co-labeled with CD31, CD45, and Sca-1, markers of NMC contaminants. Isotype Abs define gates (pink box) for negative drops without contaminants. In step 3 (S3), NMC-negative drops that also co-labeled with cTnT were positively selected for purification. Expression of cTnT is shown (far right panel) in the x-axis to demonstrate the purity of sorted MCs (green curve) vs. the pre-sort suspension (purple curve).

B, MC purity is based on the fraction of nucleated $cTnT^+$ cells from RV (red squares) and LV (green triangles) as compared to pre-sort cells (purple circles). The black dashed line is set at 95% benchmark for purity. Values are mean±SD from each ventricular preparation, numbers of samples are in parenthesis, *p* is calculated by 1-way ANOVA and Bonferroni posttest.

C, Sorted RV and LV MCs were counted in a hemocytometer to assess rod-shaped MC morphology post sort (85±9%, 50-100 MC counted per ventricle post sort, n= 10). Red scale bar denotes 100 μm. On the right graph, triplicate counts of 10-sorted cells per ventricle are shown as mean±SD. The black dashed line is set at the 92%, the precision obtained with counts. Number of sorted ventricles is in parenthesis, and *p* is calculated by Student *t* test.

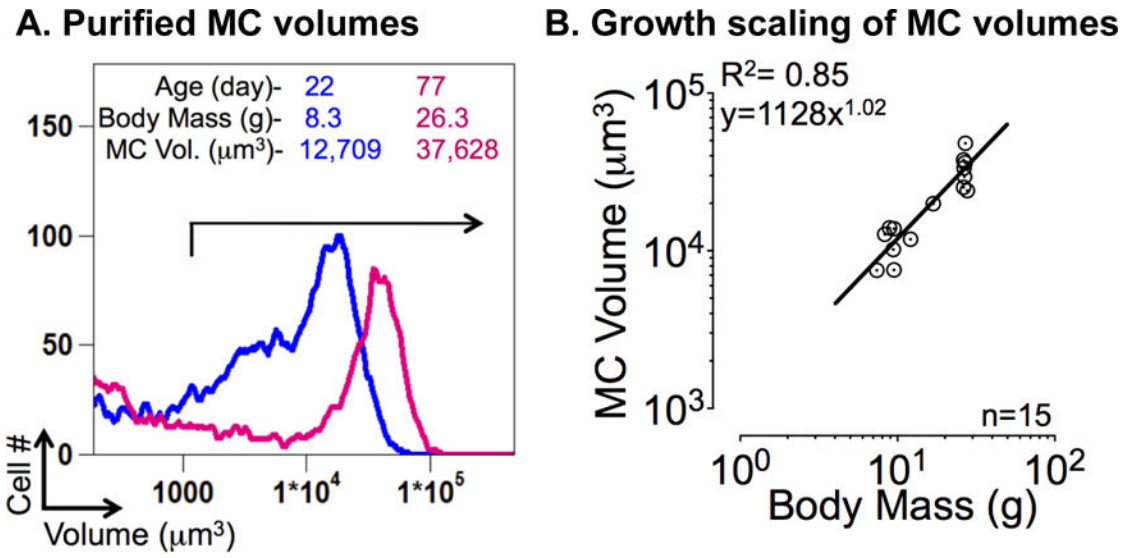

Figure 3. Myocyte size and allometric scaling

A, LP-FACS-purified MCs (10,000 per ventricle) from adult (pink curve) and weanling (blue curve) mice are analyzed with a Coulter Multisizer for cell volumes post-sort. Arrow in Coulter plot shows the MC gate used to calculate the MC median volumes. Ontogenic variables (age, body mass and MC volumes) for these two ventricles are listed in the top portion of plot.

B, Log-log bivariate plot shows the growth scaling of MC median volume in cubic microns (mm^3) vs. body mass in grams (g). Logarithmic transformation is applied to both coordinate and linearization is assessed by the best power fit to the data described by the equation $y = bx^a$, where y is the median cell volume being measured, x is body mass and a is the exponent or slope of the best straight-line known as the allometric a coefficient. The relationship R^2 is obtained by linear regression.

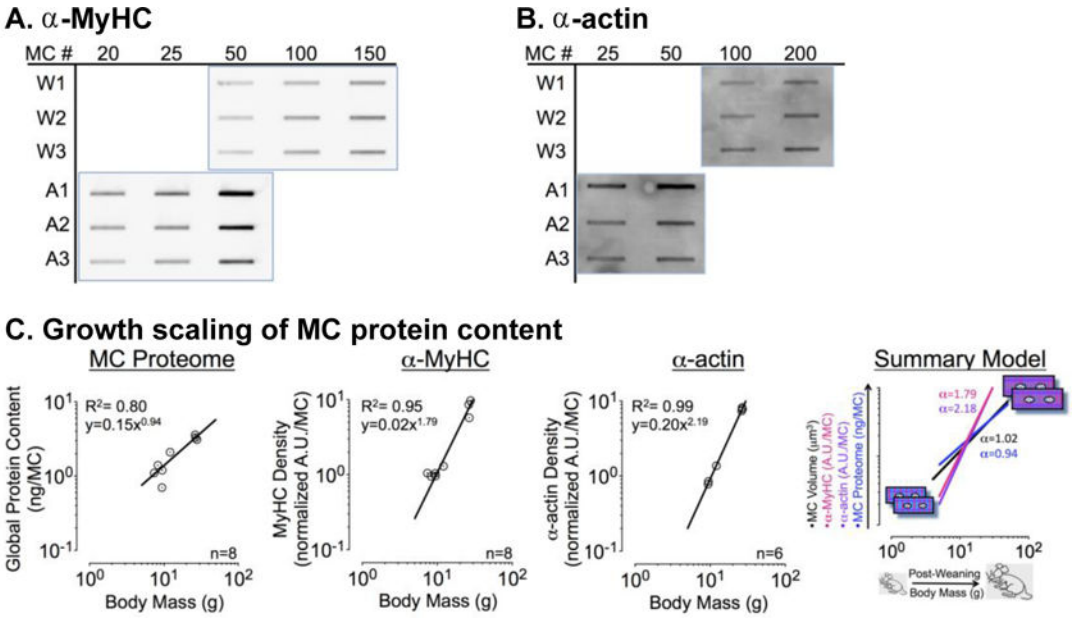

Figure 4. MC Proteome and sarcomeric protein content per-cell scaled to growth

A & B, Single slot blots were loaded with protein lysates from increasing numbers of MCs/well (MC #). Cell lysates were obtained from 10,000 purified MCs with 95% purity using LP-FACS. The number of MCs used in weanlings (W1-3) and adult (A1-3) samples vary based on signal linearity for protein densitometry (see supplemental Fig. 7). Samples are loaded in 48 well blots, and only selected regions of the blot (demarcated by blue boxes) are shown.

A, MyHC relative content is measured by immunoblotting with MF20 Ab, a total MyHC mAb primarily conjugated to HRP. Since these MCs express mostly α-MyHC, the adult isoform, the MF20 signal is representative of α-MyHC content (Fig. 1 and Supplemental Fig. 5).

B, Sarcomeric actin (α-actin) relative content is measured by immunoblotting with 5c5 Ab, an IgM mAb specific for both skeletal and cardiac muscle a-actins. Since these MCs mostly express cardiac α-actin, the adult isoform, the 5c5 signal is likely representative of this isoform.

C, The rate of MC proteome (left) and α-MyHC and α-actin (middle) accumulation per-MC is scaled to body mass, and presented in transformed log-log plots. α-MyHC and α-actin content are derived from normalized values to the average signal of weanlings in each blot. A summary of the integrated growth model (right) describes the relationship of MC-specific volume, proteome, α-MyHC and α-actin as the mouse grow during post-weaning ontogeny.